

Wave propagation along interacting fiber-like lattices

 V.I. Nekorkin^{1,2}, V.B. Kazantsev¹, D.V. Artyuhin¹, and M.G. Velarde^{2,a}
¹ Radiophysical Department, Nizhny Novgorod State University, 23 Gagarin Ave., 603600 Nizhny Novgorod, Russia

² Instituto Pluridisciplinar, Universidad Complutense, Paseo Juan XXIII, N°1, Madrid 28 040, Spain

Received 12 December 1998

Abstract. A fiber-like lattice with resistively coupled electronic elements mimicking a 1-D discrete reaction-diffusion system is considered. The chosen unit or element in the fiber is the paradigmatic Chua's circuit, capable of exhibiting bistable, excitable, oscillatory or chaotic behavior. Then the dynamics of a structure of two such interacting parallel active fibers is studied. Suitable conditions for the interaction to yield synchronization and other forms of collective behavior involving both fibers are obtained. They include wave front propagation, pulse reentry and pulse propagation failure, overcoming of propagation failure, and the appearance of a source of synchronized pulses. The possibility of designing controlled *dynamic* contacts by means of one or a few inter-fiber couplings is also discussed.

PACS. 05.45.-a Nonlinear dynamics and nonlinear dynamical systems

1 Introduction

Wave propagation in the form of pulses and other nonlinear signals along lattices is of interest to model or mimic natural phenomena [1–7]. For instance, pulse propagation along axons and synaptic transmissions constitute the dynamical basis of neuron communication, as in the transmission of an image from the retina to the visual cortex which occurs by a bundle of axons or nerve fibers [4,6,7], or in the reentry phenomena in coupled parallel fibers [8–12], etc. For a bundle of fibers an open question is the outcome of inter-fiber interaction with eventual ill-function in one or several of them. Understanding of the referred dynamics and basic phenomena can be obtained by using 1-D lattices. Thus, here we consider the drastically simple case of pulse propagation along a chain of electronic active units, in particular bi-stable elements. Since a chain represents a spatially extended system and it is capable to sustain different waves making possible transfer of an encoded information, it can be considered as an *active* “fiber”. We take Chua's circuit as the cell, unit or element in the chain. It is a paradigmatic and easy to construct nonlinear electronic device known to have a rich variety of dynamical behaviors including bistable, excitable, oscillatory and chaotic regimes [13]. We consider diffusive coupling between the cells. Thus a fiber is a discrete version of a *multi-species reaction-diffusion medium*. Indeed by varying the parameters of the electronic circuit we easily drive the “reaction kinetics”. In particular, we can mimic a bistable medium when Chua's circuit is in a simple bistable mode or an excitable FitzHugh-Nagumo

like medium when in its excitable mode and so on. Such a variety of possibilities makes the electronic fiber an effective tool to model different phenomena typical for almost all possible [4,5,10] type of RD media [13]. Accordingly, electronic experiments with arrays of coupled Chua's circuits have been done for various purposes [11,12].

Studying two coupled fibers in this paper we focus the attention on the processes of wave propagation and reentry phenomena in the system with *bistable* and *excitable* properties. Our model-problem exhibits classical wave reentry processes observed in FitzHugh-Nagumo fibers as well as some new effects caused by the complexity of the cell and by the discrete properties of the fibers [8–10]. In Section 2 we define the model problem to be considered. Then in Section 3 we show how one and two-coupled fibers behave dynamically, and we delineate the range of parameter values for fiber-fiber dynamic synchronization. Section 4 deals with the effects of such synchronization. In Section 5 the case of one or a few contacts between two fibers is considered thus illustrating features typical of synaptic-like contacts in neurons [3,4,7]. In Section 6 we summarize our findings.

2 Model

Let a fiber be a chain or 1-D lattice of N coupled electronic units as schematically shown in Figure 1. Let us also assume that the inter-fiber interaction is provided by nearest-neighbor bonds with linear resistors between the corresponding elements hence sites of the two chains. Further, let us consider two such axon-like structures coupled together. The collective dynamics of such system is described

^a e-mail: mvelarde@eucmax.sim.ucm.es

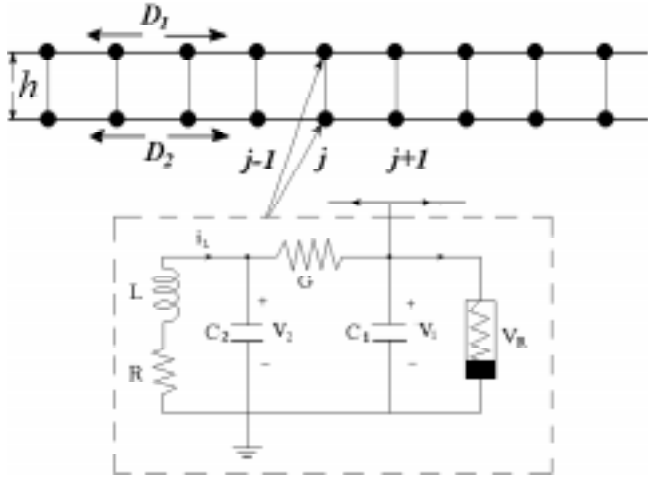


Fig. 1. Schematic diagram of the discrete two-fiber system and the active electronic unit.

by the following dimensionless coupled equations [13,14]

$$\begin{cases} \dot{x}_j^1 = \alpha(y_j^1 - x_j^1 - f(x_j^1)) + D_1 \Delta x_j^1 \\ \quad + h_j(x_j^2 - x_j^1); \\ \dot{y}_j^1 = x_j^1 - y_j^1 + z_j^1; \\ \dot{z}_j^1 = -\beta y_j^1 - \gamma z_j^1; \\ \dot{x}_j^2 = \alpha(y_j^2 - x_j^2 - f(x_j^2)) + D_2 \Delta x_j^2 \\ \quad + h_j(x_j^1 - x_j^2); \\ \dot{y}_j^2 = x_j^2 - y_j^2 + z_j^2; \\ \dot{z}_j^2 = -\beta y_j^2 - \gamma z_j^2; \end{cases} \quad (1)$$

$$j = 1, 2, \dots, N,$$

where superscripts, $i = 1, 2$, denote the variables of the first and the second fiber, respectively. The “species” x, y and z account for the voltages V_1, V_2 and the current i_L of the electronic circuit (Fig. 1 and [14]); $\Delta x_j = x_{j-1} - 2x_j + x_{j+1}$ is the discrete Laplace operator; D_1, D_2 are coefficients accounting for the strengths of the corresponding intra-fiber diffusions; h_j characterizes inter-fiber coupling (which is also of diffusive type); $f(x) = x(x - a)(x + b)$ with $a, b > 0$. Finally, Neumann or zero-flux boundary conditions are imposed on the system (1). All dimensionless parameters in (1) are expressed by the parameters of the elements of the electronic circuit [13,14]. Note that equations (1) extend the dynamic possibilities offered by the standard FitzHugh-Nagumo model [4,5].

3 Motions along a fiber and their synchronization in two coupled fibers

Let us introduce the new (difference) variables

$$\begin{aligned} u_j &= x_j^1 - x_j^2, \quad v_j = y_j^1 - y_j^2, \quad w_j = z_j^1 - z_j^2; \\ s_j &= x_j^1 + x_j^2, \quad p_j = y_j^1 + y_j^2, \quad q_j = z_j^1 + z_j^2. \end{aligned}$$

Then, the two-fiber system (1) becomes

$$\begin{cases} \dot{u}_j = \alpha[v_j - u_j - H(u_j, s_j)] + \frac{D_1 + D_2}{2} \Delta u_j \\ \quad + \frac{D_1 - D_2}{2} \Delta s_j - 2h_j u_j; \\ \dot{v}_j = u_j - v_j + w_j; \\ \dot{w}_j = -\beta v_j - \gamma w_j; \\ \dot{s}_j = \alpha[p_j - s_j - \Phi(u_j, s_j)] + \frac{D_1 - D_2}{2} \Delta u_j \\ \quad + \frac{D_1 + D_2}{2} \Delta s_j; \\ \dot{p}_j = s_j - p_j + q_j; \\ \dot{q}_j = -\beta p_j - \gamma q_j; \end{cases} \quad (2)$$

$$j = 1, 2, \dots, N,$$

with

$$H(u, s) \equiv \frac{u^2 + 3s^2}{4} + (a - b)s - ab,$$

$$\Phi(u, s) \equiv \frac{s}{4}(3u^2 + s^2) + \frac{a - b}{2}(u^2 + s^2) - abs.$$

3.1 Synchronization of two identical fibers with inter-fiber interaction

Let us first consider the case $D_1 = D_2 = D$. Then the system (2) has the trivial solution $u_j = v_j = w_j = 0$. In the phase space of (2) it defines the manifold of the synchronization of motions

$$M : \{u_j = 0, \quad v_j = 0, \quad w_j = 0\}, \quad j = 1, 2, \dots, N$$

which for suitable parameter values is globally asymptotically stable. Indeed, the quantity

$$V = \sum_{j=1}^N \left[\frac{u_j^2}{2} + \frac{\alpha v_j^2}{2} + \frac{\alpha w_j^2}{\beta} \right]$$

is a Lyapunov function. Its derivative with respect to (2) is

$$\dot{V} = - \sum_{j=1}^N [P_j + Q_j + R_j]$$

with

$$\begin{aligned} P_j &\equiv -Du_{j-1}u_j + (2D + 2h_j - \alpha(a^2 + ab + b^2)/3)u_j^2 \\ &\quad - Du_{j+1}u_j \\ Q_j &\equiv \frac{\alpha u_j^2}{2} [u_j^2 + 3s_j^2 + 4(a - b)s_j + 4(a - b)^2/3] \\ R_j &\equiv \alpha(u_j^2 - 2u_j v_j + v_j^2 + \gamma w_j^2/\beta). \end{aligned}$$

Then, all Q_j, R_j are positive definite. The function P_j is a quadratic form. It is also positive definite if

$$h_j > h^* \equiv \frac{\alpha(a^2 + ab + b^2)}{6}, \quad \forall j = 1, \dots, N. \quad (3)$$

It follows that outside the manifold M the inequality $\dot{V} < 0$ is satisfied and $\dot{V} = 0$ on the manifold. Thus, the synchronization manifold M is *globally asymptotically stable*. Therefore, any initial conditions in the identical coupled fibers tend to the manifold M where the already *synchronized* motions are governed by the system describing the dynamics of a single fiber ($h_j = 0$).

3.2 Synchronization of fibers with different diffusion coefficients and homogeneous strong inter-fiber interaction

Let us now take $D_1 \neq D_2$ with very strong inter-fiber interaction coefficients $h_j = h \gg 1$, $\forall j = 1, \dots, N$. Then, the system (2) has a small parameter, $\mu = 1/h \ll 1$, which affects the derivative \dot{u}_j . In this case the motions of (2) have both *fast* and *slow* features. In the phase space there exists a stable surface of *slow* motions defined by $\{u_j = 0, j = 1, \dots, N\}$ and all trajectories of (2) after some time become restricted within thin layers (whose thickness is of order of μ) near this surface. When $\mu = 0$ the *slow* motions are located exactly at the surface and given by the system

$$\begin{aligned} \dot{v}_j &= -v_j + w_j; \\ \dot{w}_j &= -\beta v_j - \gamma w_j; \end{aligned} \quad (4)$$

$$\begin{aligned} \dot{s}_j &= \alpha[p_j - s_j - \Phi(0, s_j)] + \frac{D_1 + D_2}{2} \nabla^2 s_j; \\ \dot{p}_j &= s_j - p_j + q_j; \\ \dot{q}_j &= -\beta p_j - \gamma q_j; \end{aligned} \quad (5)$$

where (4) and (5) describe independent systems. The system (4) is linear and all trajectories asymptotically tend to the surface $\{v_j = w_j = 0, j = 1, \dots, N\}$. Thus, the slow motions occur on the surface that *coincides* with the synchronization manifold M . The dynamics on this surface is given by the system (5) describing a single chain with diffusion coefficient $D_s = (D_1 + D_2)/2$. Hence, for $h \gg 1$ evolution proceeds in two stages. Any initial condition in the first (fast) stage quickly comes to the thin layer which is very close to the stable surface of slow motions (synchronization manifold M). In the second (slow) stage, motions are governed approximately by the system (5) defining the dynamics of the single chain with $D = D_s$ and tend to an attractor of this system (for example, a steady state or a wave pattern).

4 Effects of inter-fiber interaction for varying “reaction kinetics”

In the preceding section we have analytically found a sufficient condition for the synchronization of all possible motions in the two coupled fibers. Let us now see concrete effects of the inter-fiber interaction. To do this we numerically integrate the equations (1) for different modes (*i.e.* various possible “reaction kinetics”) of the unit and for varying intra-fiber diffusion. We restrict consideration to the homogeneous case, $h_j \equiv h$.

4.1 Wave fronts in coupled interacting fibers

Let us choose the parameters of the electronic circuit such that it possesses two stable steady states. Let us take $\gamma \gg 1$. In this case each fiber can be approximately described by a gradient system [14]. In particular, the dynamics of each unit is given by

$$\begin{cases} \dot{x} = -\alpha \frac{\partial U(x, y)}{\partial x} \\ \dot{y} = -\frac{\partial U(x, y)}{\partial y} \end{cases} \quad (6)$$

with the potential

$$U(x, y) = \frac{x^4}{4} - \frac{(a-b)x^3}{3} - \frac{(ab-1)x^2}{2} + \frac{y^2}{2} - xy. \quad (7)$$

The two stable steady states of the unit correspond to the two minima of the potential. Then, a single fiber represents a discrete *bistable*, reaction-diffusion system of FitzHugh-Nagumo type. Increasing the diffusion coefficient $D > D_{fr}$ above some critical value D_{fr} such a fiber exhibits wave front propagation. A front is formed as a consequence of the transition of the units to the state with lower value of the potential function U . Thus, for fixed D the direction of front propagation and its velocity are uniquely defined by the difference in the potential levels between the two minima of U . Let us show that when the fibers are coupled, $h \neq 0$, there is the possibility of dramatically changing the properties of propagating fronts.

In the numerical calculations we fix the parameters of the cell to $a = 1.4, b = 1.8, \beta = 0.5, \alpha = 1$ and $\gamma = 10$, hence for all practical purposes $\gamma \gg 1$. This set of parameter values provides the required properties for the cell to be a *bistable* unit.

4.1.1 Synchronization of traveling wave fronts

Let us consider $D_1 = D_2 > D_{fr}$ and let the initial conditions be two fronts propagating in the same direction along parallel fibers with a finite time delay (Fig. 2, $t < t_0$). The level of grey color corresponds to the value of x in the junctions of the chains according to the map given in the figure. Sudden switching of the inter-fiber interaction at $t = t_0$ makes the delay negligible after a transient process (Fig. 2, $t_0 < t < t_1$). Then the fronts become synchronized and propagate together (Fig. 2, $t > t_1$). When the fronts hit the boundary a steady homogeneous distribution appears in the fibers, hence each unit comes to the lower minimum of the potential U , marked by white color. The transient process in Figure 2 occurs in the following way. The front in the first fiber, arriving with delay, significantly increases its velocity while the first arriving front in the second fiber reverses motion and travels backward.

To describe these effects (front acceleration and front reversal) let us consider the gradient model (6). Let us take the front in the first fiber propagating relative to one

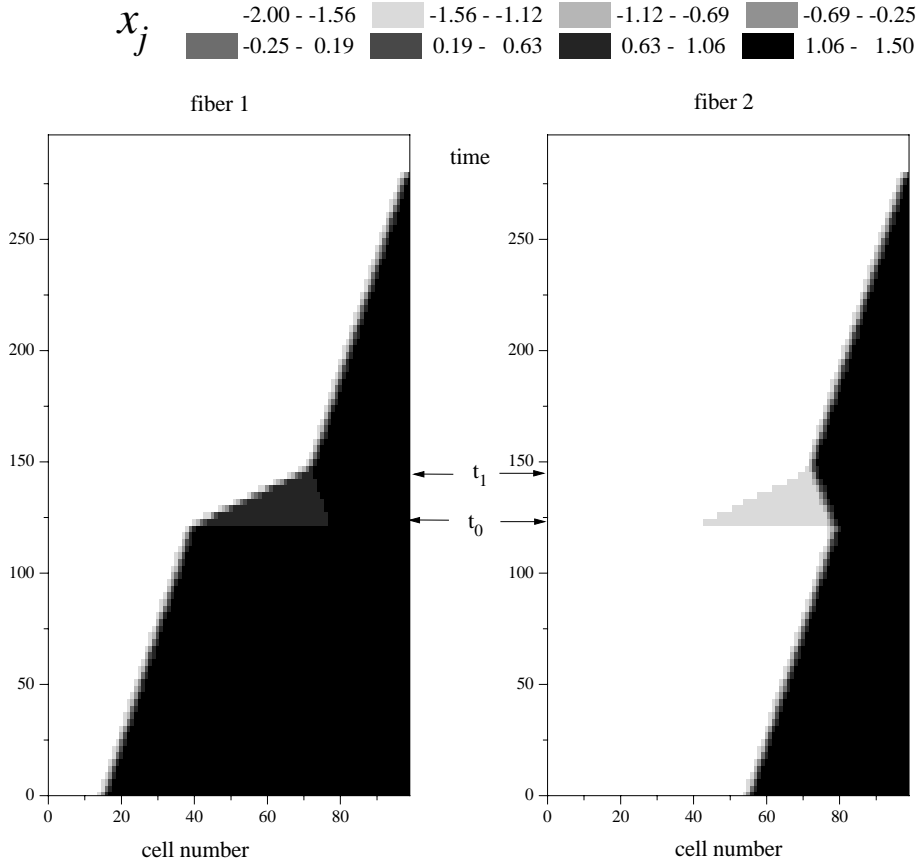


Fig. 2. Wave fronts in two identical bistable fibers with $D = 2$. (a) Synchronization of two wave fronts traveling with finite time delay. For $t < t_0 = 120$ the chains are independent, $h = 0$. At $t = t_0$, the interaction is switched-on, $t > t_0$, $h = 0.5$. The time interval $t_0 < t < t_1 \approx 140$ corresponds to a transient process. Vertical axes account for time in arbitrary units (a.u.).

of the two accessible homogeneous states in the second fiber. The inter-fiber interaction just slightly affects the homogeneous state of the second fiber. Hence, approximately, the influence of the second fiber can be estimated as a constant in the difference term of equations (1), *i.e.*

$$h(x_j^2 - x_j^1) \approx h(x_0 - x_j^1)$$

where x_0 is an x -coordinate of the steady homogeneous state. It takes the values $x_0 = a$ and $x_0 = -b$ for the two states. Then, the units of the first fiber are described by the model (6) with the *effective* potential function

$$U_h(x, y) = U(x, y) + \frac{h}{2\alpha}(x_0 - x)^2.$$

Figures 3a, 3b illustrate cross-sections of the surface $U_h(x, y)$ by the plane $y = x$ for the values of x_0 corresponding to the steady states with lower (at $x_0 = -b$) and higher (at $x_0 = a$) potential levels, respectively. The potential function $U(x, y)$ for the units of the single fiber is shown by the dashed curve. In Figure 3a the difference in the potential levels between the two minima increases (the right minimum practically disappears), hence the front should increase its velocity. It is what we have seen in Figure 2 in the first fiber. Figure 3b shows that when x_0 is associated with the state of higher potential

($x_0 = a$), the left minimum of the U_h goes up. Then, the backward transition of the cell from the left minimum to the right becomes energetically preferable. Hence, there is the reversal of wave fronts in the coupled fibers (the second fiber in Fig. 2).

4.1.2 Overcoming propagation failure in coupled fibers

Another example of the effect of inter-fiber action allowing to change qualitatively the behavior of the coupled fibers as a whole is the possibility to overcome front propagation failure.

The existence of a huge number of stable steady patterns in discrete chains with *bistable* kinetics, when D is small enough, leads to wave front propagation failure [14–19]. The perturbation of a front is always “pulled” by one of the stable steady patterns, hence fails to propagate. This leads to the failure in the functioning behavior of the fiber as a transfer system.

Let us take one chain with $D_1 > D_{fr}$ such that it allows front propagation and the other chain with $D_2 < D^*$ is the ill-functioning fiber where waves fail to propagate. D^* is some given value not needed explicitly here. As shown in Section 3.2, with strong enough inter-fiber interaction,

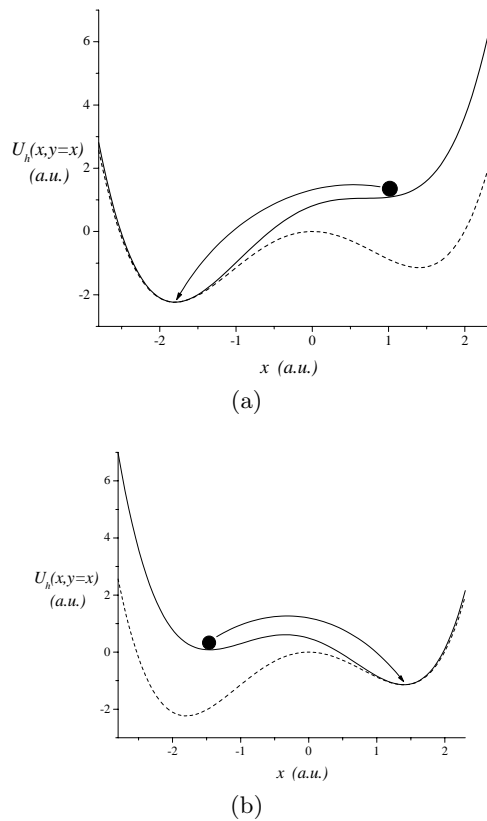


Fig. 3. Effective potential functions, U_h , for the coupled fibers describing (a) front acceleration and (b) front reversal propagation. Units are arbitrary (a.u.).

$h \gg 1$, all motions in the fibers come very close to be synchronized. They are restricted within a thin layer near the synchronization manifold M where both fibers behave, approximately, as a single one with the mean diffusion coefficient $D_s = \frac{D_1 + D_2}{2}$. Hence, if we choose D_1 large enough, $D_s > D_{fr}$, the propagation failure in the ill-functioning fiber is overcome. This effect is illustrated in Figure 4. When the fibers are independent ($t < t_0$) there is a wave front in the first one (well-functioning fiber) and a stable steady pattern in the second one (ill-functioning fiber). The strong interaction between the fibers is switched-on instantly at t_0 . After a very short transient process (fast motion stage) the steady pattern disappears in the ill-functioning fiber and there arises a wave front almost identical to the front propagating in the first fiber ($t > t_0$). Note that the velocity of the synchronized fronts is lower than the velocity of the original front. This is due to the inequality $D_s < D_1$ and to the fact that the typical dependence of front velocity on diffusion strength in a reaction-diffusion system is generally an increasing function [14].

4.2 Synchronization in coupled excitable fibers

Another possible “reaction-kinetics” of the unit allows a fiber mode with *excitable* properties [11,20]. Such is the

case for a chain ((1), $h_j = 0$), when $a = b = 1.4, \gamma = 0.01, \beta = 0.5$. We take α as a control parameter. Then, the chain sustains the propagation of stable solitary pulses or complex pulse trains.

The dynamics of excitations in systems of fibered or layered spatial architecture is of great importance in biology. In particular, excitation reentry in cardiac tissue is known to be responsible for several types of arrhythmia in heart. In a number of recent papers [8–10] a model of two coupled fibers of FitzHugh-Nagumo type has been considered. Phenomena of different types of reentry of propagating, action potential-like pulses have been studied. References [11,12] devoted to experiments with coupled linear arrays composed of cells like those considered here show the potential of studying the reentry in discrete electronic fibers.

Let us study now the dynamics of pulse-like excitations. We focus attention on the reentry phenomena as a result of the inter-fiber synchronization. It appears that pulse-like excitations as well as the reentry typical for the classical FitzHugh-Nagumo type models and quite different effects of initiations of pulse bound states or traveling “bursts” are possible.

4.2.1 Simple pulse reentry and pulse failure

Let a single pulse be propagating in one fiber as an excitation of the rest state, while the second fiber is in the rest state. When the inter-fiber interaction occurs instantaneously at a given instant of time, the fibers tend to be synchronized. Indeed, a pulse completely identical to the initial one can be excited in the second fiber and the two pulses synchronously travel down to the bottom of the fibers. We have the simple “entry” of the excitation fiber into the fiber originally in its rest state. The situation is similar to that observed in fibers of FitzHugh-Nagumo type [8] when the excitation threshold in the second fiber is low enough. The pulses may also *fail* to propagate in the coupled fibers as a result of the inter-fiber synchronization. In this case the pulse in the first fiber disappears and both chains come to the rest state. Apparently, the pulse is “pulled” by the second fiber at rest which demands a higher threshold to be excited. At variance with the failure in chains, with simple *bistable* “kinetics”, where failure is caused by ill-functioning behavior, here pulse propagation failure in the coupled fibers comes from the destruction of a given original excitation, while both fibers stay well-functioning.

4.2.2 Initiation of trains of pulses

A single fiber allows a variety of complex wave solutions steadily translating along it [20]. In particular, one can easily excite pulse trains or *bound* states composed of an arbitrary number of humps or “spikes”. Here we show how such bound states appears as a result of pulse reentry in coupled fibers.

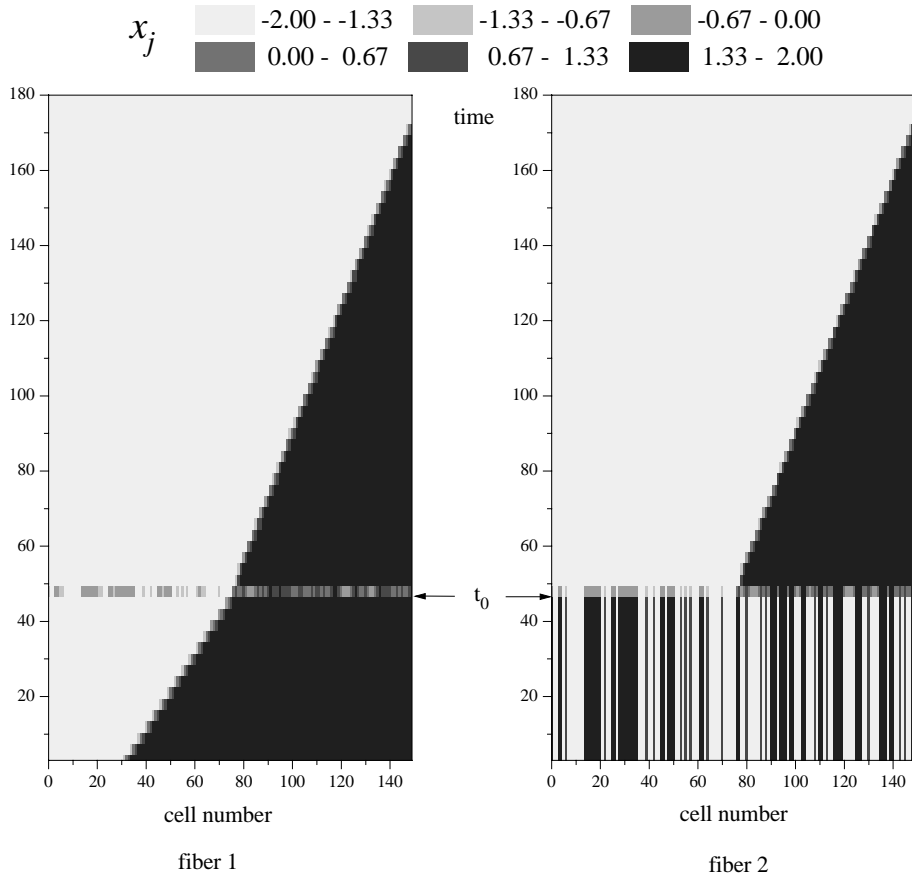


Fig. 4. Propagation failure overcome in coupled *bistable* fibers. Diffusion coefficients: $D_1 = 3$, $D_2 = 0.2$. At $t_0 = 48$ the inter-fiber interaction is switched-on, $h = 10$. Vertical axes account for time in arbitrary units (a.u.).

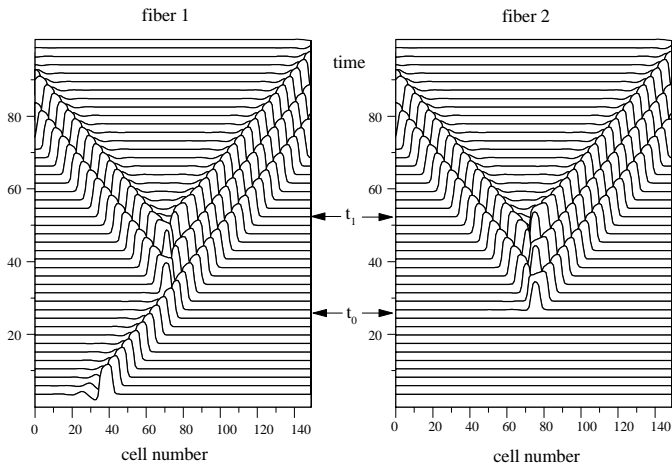


Fig. 5. Long lasting pulse source generating trains of pulses. Parameter values: $\alpha = 4.5$, $D = 2$, $h = 1.05$, $t_0 = 25, t_1 \approx 52$. Vertical axes account for time in arbitrary units (a.u.).

The appearance of synchronized trains of pulses (bound states) traveling in opposite directions can be observed as follows. After the interaction is switched-on there appears a “long lasting transient source of pulses” which may generate two- or more pulses (multi-hump pulse) identical for both fibers (Fig. 5). Note, that in this

case the coupling coefficient h should be taken smaller than the predicted synchronization threshold (3). Thus the inter-fiber interaction looks more “elastic” but still enough to synchronize the chains. Further decreasing the coefficient h leads to the appearance of a long lasting pulse source.

To illustrate how the two-fiber system exhibits such pulse trains we introduce the quantity characterizing how the system reaches the synchronization manifold

$$dist(t) = \frac{\sqrt{\sum_{j=1}^N (u_j^2(t) + v_j^2(t) + w_j^2(t))}}{3N} \quad (8)$$

which is a distance between the vectors of the two chains in a $3N$ -dimensional state space. Its vanishing value corresponds to the complete synchronization of the fibers. Figure 6 shows the time evolution of the function for three different values of h . When (3) is fulfilled (e.g. $h = 5$) the distance monotonically vanishes. This is the case of a “rigid” interaction when the system takes either the pulse or the rest state in the second fiber. For lower values of h we have more “elasticity” in the interaction and $dist(t)$ has rather long lasting oscillations associated with the appearance of the source of pulses. After some time the source dies out and the distance between the dynamic

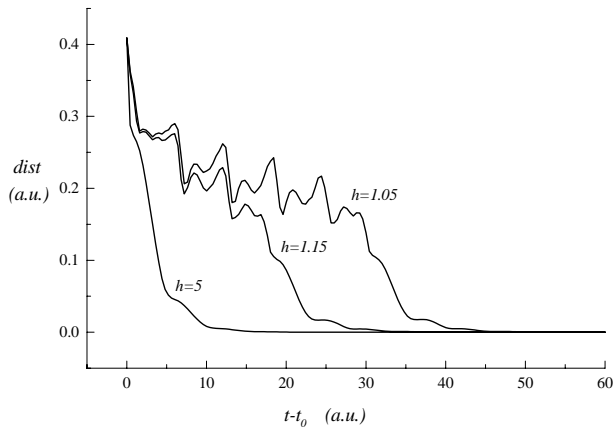


Fig. 6. Controlled distance, $dist$, as a function of time for three different values of the inter-fiber interaction. The curves illustrate that synchronization is indeed achieved. Units are arbitrary (a.u.).

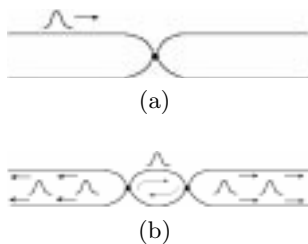


Fig. 7. Schematic diagram of two parallel fibers coupled by (a) a single-pin contact and (b) a double-pin contact.

states in the two fibers tends to zero (Fig. 6). In this case mutually synchronized bound states appear. By varying h we have the possibility to control the number of humps or spikes in the pulse train. This number is also sensitive to the values of the other parameters of the system and to changes in the initial conditions.

At variance with the cycle mechanism of pulse reentry in coupled *excitable* fibers resulting in the appearance of a sequence of pulses [8–10] the initiation of pulse trains or bound states can not be explained in simple terms of sequential excitation entry from fiber to fiber. Rather, it has to do with the possibility of stable propagation of trains (bound states) with variable number of spikes and with the oscillatory properties of a single fiber. In particular, a pulse initiating the reentry has a remarkable oscillatory tail whose “oscillations” tend to grow when the inter-fiber interaction occurs and hence to form a number (controlled by h) of spikes of the outcoming pulse trains.

5 Pulse driving by pinned inter-fiber contacts

Let us, finally, consider the case when the inter-fiber interaction operates with one or a few contacts between the two chains, hence the vector $\{h_j\}$ has only a few non-zero components (Fig. 7). Such contacts can be easily realized with discrete electronic chains [12].

5.1 Single pin contact

Let two identical fibers be connected at a single point, $h_j = h$, $h_k = 0$, $\forall k \neq j$, with h strong enough (Fig. 7a). It follows from the equations (2) that for strong enough interaction, $h \gg 1$, the difference $\dot{u}_j \sim -2hu_j$ in this pair tends to decrease and vanish. Hence the two coupled units of the different fibers tend to be synchronized (at least their x variables). Similarly to the case of the homogeneous inter-fiber coupling (Sect. 4) such a synchronization process takes time, *i.e.*, it is a transient process whose duration depends on the particular value of the coefficient h . Hence, we have, in fact, a *dynamic contact* between the parallel fibers acting with its own time scale. Two possible results of such a contact are that the pulse reaching the contact in Figure 7a dies out for large enough inter-fiber coupling, hence the contact operates as a barrier for excitation transmission, or, alternatively, at the contact point the excitation “enters” the fiber at rest where two new pulses appear. In the last case, occurring for small enough inter-fiber coupling, the forward traveling pulse propagates almost synchronously with the original pulse which also propagates in the first fiber. Thus, depending on its strength the dynamic contact acts in two different ways. It either stops the pulse thus *inhibiting* transmission or it allows the pulse to go over which is an *excitatory* action on the next chain element.

The phenomena of pulse driving in the pinned contact can be interpreted in terms of characteristic time scales of the contact operating, T_c , and the diffusion action, T_p , accounting by the pulse velocity. Let us look at the interaction process from the spatial site of the chain where the interaction occurs. Roughly, the pulse propagating in the first fiber can be splitted into several independent “portions” that sequentially bring excitation to those coupled units which are in the rest state. When a portion comes to the site of contact the interaction operates in two steps: (i) The two coupled units become synchronized very rapidly (h has a rather large value); (ii) the synchronous evolution of the coupled pair defined approximately by the dynamics of the single unit brings the coupled pair to the rest state, hence tends to kill the original excitation. These two steps account for the characteristic time of the contact action, T_c . Thus, if this interval of time is much smaller than the time, T_p , needed for the excitation to reach the units nearest to the site of contact in the two fibers, $T_c \ll T_p$, then the “portions” of the pulse sequentially die at the contact. This inhibits a further pulse propagation. But if when the contact is operating the excitation has enough time to be transmitted by diffusion to the nearest units, $T_c \gg T_p$, hence to excite them, the pulse overcomes the contact site in the first fiber, and two pulses are excited in the fiber at rest. Note that for fixed parameter values of the unit, the time scale, T_p , is estimated from the pulse velocity c , $T_p \sim 1/c$. The dependence of c on the diffusion coefficient, D , in discrete reaction-diffusion systems [14, 20] is typically $c \sim \sqrt{D}$, hence $T_p \sim D^{-\frac{1}{2}}$. The time scale T_c depends only on the value of h and decreases with $h \rightarrow \infty$ to some constant value T_0 accounting the second step (ii) of the contact action.

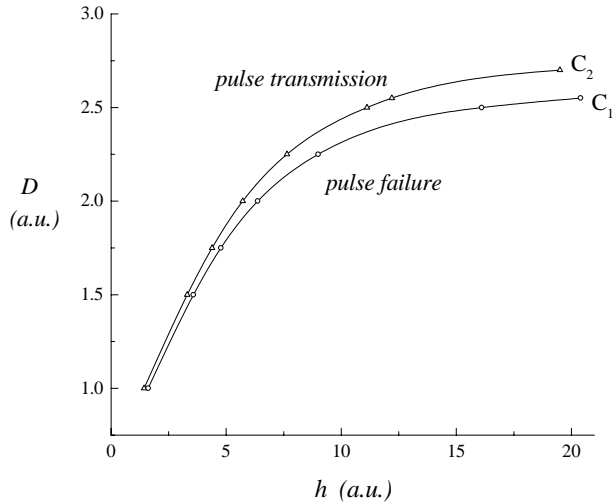


Fig. 8. Diagram of pulse driving by single-pin contact in (D, h) parameter plane. The pulse fails to propagate for values chosen below the curve C_1 . Above the curve C_2 the pulse successfully overcomes the contact. Units are arbitrary (a.u.).

It is difficult to, quantitatively, estimate these time scales because of the complex internal dynamics of the unit. To illustrate the relative action of the two time scales Figure 8 provides the diagram of pulse driving in the (D, h) parameter plane obtained numerically. In the region below the curve C_1 the contact yields pulse failure. Above the curve C_2 the pulse overcomes the contact and excites (for a certain value of h) the second fiber. The region between C_1 and C_2 corresponds to the complex outcome of the system. Here the time scales T_c and T_p become comparable and the result of the contact action crucially depends on the nontrivial dynamics of the unit. In particular, complex wave structures including pulses and wave fronts may appear.

Such behavior of a dynamic contact is not alien to what is known about synaptic linkages connecting an axon with dendrites in another neuron [3, 6, 7]. Similarly to synapses our dynamic contact is acting only when an excitation reaches it. Then, the excitation transfer occurs in the dynamic contact with a finite time delay very much like that needed by neurotransmitters to bring an excitation into the post-synaptic cell. The synaptic contacts of nerve cells may be excitatory, hence firing the post-synaptic cell, or inhibitory, hence propagation failure. Our dynamic contact shows both these synaptic features.

5.2 Double pin contact

Let us now consider the situation when the *excitable* fibers have two dynamic contacts (Fig. 7b). In this case the vector $\{h_j\}$ has two non-zero components. Let us assume them to be “elastic” contacts allowing pulse entry (Sect. 5.1). Such contacts allow the reentry of pulses from fiber to fiber. Figure 9 illustrates the space-time diagram of such system. The initial pulse put between the contacts is shown by dashed lines. When the pulse passes over the

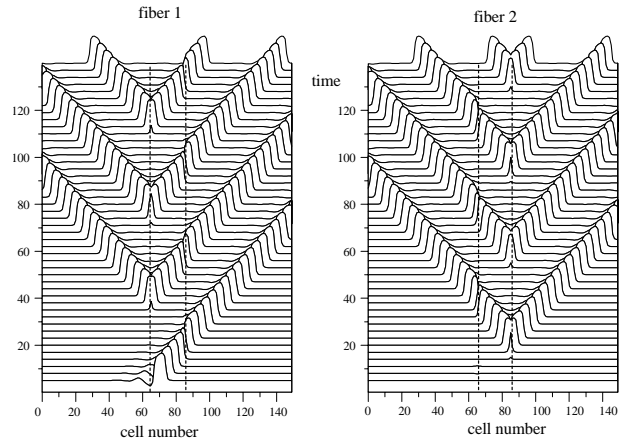


Fig. 9. A generator of synchronized pulses when the parallel excitable fibers have two-pin contacts. Parameter values: $\alpha = 4.5$, $D = 2$, $h_{65} = h_{85} = 5$. Vertical axes account for time in arbitrary units (a.u.).

left contact two new pulses appear in the second fiber. One of them traveling backward reaches the right contact and in turn two other new pulses are excited in the first fiber. Consequently, a sequence of pulse reentries may occur. Two sequences of almost synchronized pulses occur at both ends of the fibers as shown in Figure 9. Thus, the system represents, in fact, a spatially extended generator of synchronous pulses (Fig. 7b).

Note, that the outcome of the system (Fig. 9) is similar to the cycle reentry observed in FitzHugh-Nagumo fibers [8] where the sequential reentry of excitation from fiber to fiber is defined only by the characteristic refractory period. However, in our case the extended generator acts stationary and the time lapse or period between the pulses can be controlled at will by suitably placing the dynamic contacts at different sites of the two chains.

6 Conclusion

We have investigated the phenomena of pattern and wave or pulse interaction in a system of two coupled fiber- or axon-like, 1D lattices. In particular, we have considered fibers composed of electronic units resistively coupled. The choice of the unit has been dictated by the paradigmatic nature of Chua’s circuit [13]. Indeed by varying its parameter values it has been shown that this electronic element may exhibit bistable, multistable, excitable, oscillatory and chaotic behavior. Thus it represents a significant extension of the dynamic possibilities offered by the standard FitzHugh-Nagumo model [4, 5]. It has been analytically proved, and numerically verified, that for strong enough inter-fiber coupling the possibility of mutual synchronization of all motions is actually realized. We have also, numerically, illustrated how the inter-fiber coupling can lead to nontrivial, synergetic effects in the spatio-temporal dynamics of the coupled fibers. The reversal in the propagation of a wave front, growth of front velocity, pulse reentry and pulse failure, overcoming of propagation failure and the appearance of sources

of pulses are a few spectacular possibilities of the model-system here studied.

We have also described the results of interaction between parallel fibers with one and two inter-fiber connections. Such architecture represents an effective tool of pulse driving in parallel fibers. In particular, pinned coupling between the fibers brings controlled transfer of an excitation from one fiber to the other. Such a contact mimics synaptic connections between neurons [3,7]. Fibers with two dynamic contacts can operate as a spatially extended generator of synchronous sequences of pulses with controlled time delay between them.

We have shown the really good agreement of the results obtained with known results for excitable fibers of FitzHugh-Nagumo type [4,5,10]. Thus the two coupled electronic fibers studied here provide a reliable model to simulate different reentry phenomena observed in many natural systems.

The authors have benefited from fruitful discussions with Professors H. Haken, L.O. Chua, G. Nicolis, A. Fdez de Molina, R.R. Llinas and F. Werblin. This research has been supported by the BCH Foundation (Spain), by the Russian Foundation for Basic Research under Grant 97-02-16550, by the program "Soros Post Graduate Students" under Grant a97-853 (Russia), by NATO under Grant OTR LG96-578, by EU under Network Grant 96-10 and by DGICYT (Spain) under Grant PB96-599.

References

1. A. Scott, *Active and Nonlinear Wave Propagation in Electronics* (Wiley Interscience, N.Y., 1970).
2. H. Haken, *Information and self-organization* (Springer-Verlag, Berlin, 1988).
3. H. Haken, *Principles of brain functioning* (Springer-Verlag, Berlin, 1996).
4. V.S. Markin, V.F. Pastushenko, Y.A. Chizmadzhev, *Theory of excitable media* (John Wiley & Sons, N.Y., 1987).
5. J.D. Murray, *Mathematical Biology*, Second Corrected Edition (Springer-Verlag, Berlin, 1993).
6. D.H. Hubel, *Eye, brain and vision* (W.H. Freeman and Company, N.Y., 1995).
7. *The Biology of the Brain. From Neurons to Networks*, edited by R.R. Llinas (W.H. Freeman and Company, N.Y., 1988).
8. A. Palmer, J. Brindley, A.V. Holden, *Bull. Math. Biology* **54**, 1039 (1992).
9. A.V. Panfilov, A.V. Holden, *Phys. Lett. A* **147**, 463 (1990).
10. J. Brindley, A.V. Holden, A. Palmer, *Nonlinear Wave Processes in Excitable Media*, edited by A.V. Holden, M. Markus, H.G. Othmer (Plenum Press, N.Y., 1991).
11. I. Perez Marino, M. de Castro, V. Perez-Munuzuri, M. Gomez-Gesteira, L.O. Chua, V. Perez-Villar, *IEEE Trans. Circ. Syst.* **42**, 665 (1995).
12. M. de Castro, M. Gomez-Gesteira, V. Perez-Villar, *Phys. Rev. E* **57**, 949 (1998).
13. R.N. Madan, *Chua's circuit: a Paradigm for Chaos* (World Scientific, Singapore, 1993).
14. V.I. Nekorkin, L.O. Chua, *Int. J. Bifurc. Chaos* **3**, 1282 (1993).
15. T. Erneux, G. Nicolis, *Physica D* **67**, 237 (1993).
16. D.M.W. Leenaerts, *Proc. Int. Symp. NOLTA'97* (1997), p. 257
17. V. Perez-Munuzuri, V. Perez-Villar, L.O. Chua, *J. Circuits, Syst. Comput.* **3**, 215 (1993).
18. J.P. Keener, *SIAM J. Appl. Math.* **47**, 556 (1987).
19. A.R.A. Anderson, B.D. Sleeman, *Int. J. Bifurc. Chaos* **5**, 63 (1995).
20. V.B. Kazantsev, V.I. Nekorkin, M.G. Velarde, *Int. J. Bifurc. Chaos* **7**, 1775 (1997).
21. V.I. Nekorkin, V.B. Kazantsev, M.G. Velarde, L.O. Chua, *Phys. Rev. E* **58**, 1764 (1998).